Molecular beam epitaxy of InP-based alloys for long-wavelength vertical cavity lasers

David A. Buell[a)]
Department of Materials, University of California, Santa Barbara, California 93106

Daniel Feezell
Department of Electrical and Computer Engineering, University of California, Santa Barbara, California 93106

Bjørn-Ove Finland[b)]
Department of Electrical and Computer Engineering, University of California, Santa Barbara, California 93106

Larry Coldren
Department of Materials, University of California, Santa Barbara, California 93106 and Department of Electrical and Computer Engineering, University of California, Santa Barbara, California 93106

(Received 14 September 2005; accepted 3 April 2006; published 30 May 2006)

In this article we describe the growth, design, and characterization of a 1310 nm lattice-matched vertical cavity laser which take advantage of an AlGaAsSb distributed Bragg reflector and AlInGaAs active regions. The molecular beam epitaxial growth for this structure was particularly challenging due to the various III–V alloys used; in particular, the interfaces between them were observed to be a significant source of macroscopic defects and roughness. The AlGaAsSb–InP interface was seen to control the yield and overall quality of device structures, and so was the focus of the crystal growth optimization. InP heat- and current-spreading layers were utilized to offset the thermal and electrical limitations of the AlGaAsSb mirrors; we optimized the defect density and roughness of these epilayers by studying their dependence on growth temperature and P overpressure. Vertical cavity lasers grown using these optimized approaches and incorporating a thin, selectively etched tunnel-junction aperture were fabricated and tested, and demonstrated promising characteristics. Operating temperatures up to 90 °C with single-mode power in excess of 1.6 mW were observed. Differential quantum efficiency of 64% was seen for our best devices, a record for long-wavelength vertical cavity lasers. © *2006 American Vacuum Society.*
[DOI: 10.1116/1.2200380]

I. INTRODUCTION

Vertical cavity lasers (VCLs) operating in the wavelength space from 1300 to 1600 nm are interesting data communication and telecommunication sources for existing fiber-optic networks, since they take advantage of absorption and dispersion minima in conventional silica fiber; their circular output mode shape, low dissipated power, and efficient direct modulation behavior make them favorable for network applications. VCLs operating at shorter wavelengths (780–980 nm) have demonstrated excellent performance characteristics for short distance communications.[1] In order to translate these successes to the local-, storage-, and metroarea networks, VCLs operating at 1310 and 1550 nm are desired. There have been two general lines of approach for realizing long-wavelength VCLs to this point: GaAs based and InP based. GaAs-based approaches take advantage of AlGaAs/GaAs distributed Bragg reflectors (DBRs) with their associated high index of refraction contrast and thermal conductivity. The optical and current aperturing technology is also well developed, with submicron devices incorporating tapered oxide apertures demonstrating high-speed modulation and high differential quantum efficiency. In order to extend the operation of GaAs-based devices from 980 to 1310 and 1550 nm, less mature active region materials such as GaInN(Sb)As or InGaAs quantum dots must be used.[2,3] These active regions are relatively new, and their reliability at longer wavelengths remains in question.

InP-based approaches take the opposite tack: the active region materials, AlInGaAs and InGaAsP, are well developed, having been deployed in commercial long-wavelength edge-emitting lasers for many years. The DBR and aperturing technology, however, are less well developed. The conventional lattice-matched alloys to InP, AlInGaAs, and InGaAsP do not have sufficient index contrast to be effective options for DBRs with high reflectivity. This has led to a variety of approaches to realize InP-based VCLs, including wafer-fused AlGaAs/GaAs DBRs,[4] metamorphically grown AlGaAs DBRs,[5] and dielectric DBRs.[6] Devices with high operating temperature, useful output power, and good differential efficiency have been demonstrated using each of these techniques.

[a)]Electronic mail: dave.buell@gmail.com
[b)]On leave from Department of Electronics and Telecommunications, Norwegian University of Science and Technology, NO-7491 Trondheim, Norway.

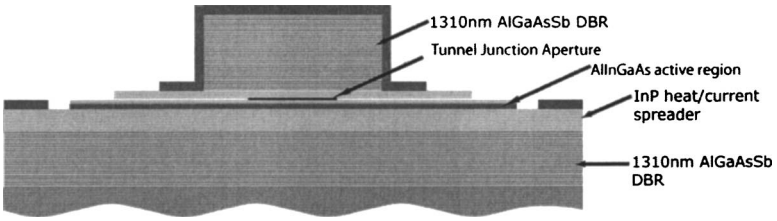

FIG. 1. Vertical cavity laser at 1310 nm with AlGaAsSb mirrors and AlInGaAs active region, with thin AlInGaAs tunnel-junction aperture for current and optical confinement.

In this article we report the results using an alternative approach, in which we take advantage of the InP lattice-matched material AlGaAsSb. Our group has reported VCLs based on this technology before, both at 1550 nm (Ref. 7) and more recently at 1310 nm.[8] Prior results at 1550 nm showed operating temperature of 88 °C and 1.2 mW output power at 15 °C, with 23% differential quantum efficiency. Improvements to the device design and epitaxial growth have led to our most recent results, in which 1310 nm VCLs have been fabricated which operate to 90 °C, have 1.6 mW single-mode output power, and a record differential quantum efficiency of 64%. The molecular beam epitaxial growth optimization is detailed below.

II. MOLECULAR BEAM EPITAXY

The vertical cavity laser structures detailed in this article were grown using molecular beam epitaxy in a Varian Gen-II reactor, with standard EPI-SUMO effusion cells for group III elements and valved, cracked sources for all group V elements. For our laser structures, AlGaAsSb alloys were used as DBRs, AlInGaAs was used for active regions and tunnel junctions, and InP for heat- and current-spreading layers. The optimization of these different alloys, as well as the interfaces between them, was of utmost importance to successful device fabrication. A schematic of a fully fabricated VCL is given in Fig. 1 to illustrate the relationship between the various alloys and their placement in the device structure.

A. AlGaAsSb DBR growth

Lattice-matched $AlAs_{0.56}Sb_{0.44}$ and $GaAs_{0.51}Sb_{0.49}$ has been demonstrated to be a suitable candidate for DBRs in the wavelength span of 1310–1550 nm.[9] We controlled the composition of the AlGaAsSb alloy via short-period superlattices (2.0 nm) with varying duty cycles of AlAsSb and GaAsSb. Using this method we formed alternating 1/4 λ layers of $Al_{0.95}Ga_{0.05}As_{0.54}Sb_{0.46}$ and $Al_{0.30}Ga_{0.70}As_{0.52}Sb_{0.48}$, referred to in this article as 95%AlGaAsSb and 30%AlGaAsSb, respectively. Growth was performed at a temperature of 480 °C as measured using an Ircon optical pyrometer, and a growth rate of 0.35 nm/s. The lattice matching of the ternaries was achieved using the method we have previously reported, in which the beam flux ratio for As/Sb is fixed to ~6.5, and fine-tuning of the composition was done by adjusting the Al and Ga beam fluxes.[10] Stable lattice-matched conditions were possible using this method, with observed x-ray diffraction (XRD) peaks indicating less than 0.01% strain in the growth direction. Minimum defect density and roughness, as measured using atomic force microscopy (AFM), for samples grown using the above parameters were 150 cm^{-2} and 0.17 nm rms, respectively. The bottom (output) DBR for the 1310 nm VCL consisted of 27.5 pairs, while the top (highly reflective) DBR used 39.5 pairs.

B. InP growth diagram

Homoepitaxy of InP, compared to GaAs, has a narrow optimal growth window. Previously we had observed that the defect density in our bulk layers of InP was sufficient to increase optical losses and thus decrease device performance. An investigation of the InP growth diagram for our conditions was thus necessary. We have previously found that InP substrate orientation played a large role in the quality of subsequently grown InP epilayers, with optimum films observed on (001) substrates miscut 0.5° towards the (111)*A* planes. For compatibility with the other requirements of our system, an InP growth rate of 0.15 nm/s was fixed, and other pertinent growth parameters were varied. In Fig. 2 we present the dependence on growth temperature and P_2 beam flux pressure of the macroscopic defect density and rms roughness. In these experiments an InP growth rate of 0.15 nm/s was achieved using an In beam flux of 3.6×10^{-7} Torr.

Growth of InP under 9×10^{-6} Torr P_2 overpressure at a temperature of 465 °C yielded films with defect density equal to 200 cm^{-2} and rms roughness of 0.17 nm for 1 μm thick epilayers. InP which was grown on the optimized AlGaAsSb DBRs described above, however, suffered from increased defect density and roughness. In order to grow the highest quality devices an investigation into the interface between AlGaAsSb and InP was necessary.

1. AlGaAsSb–InP interface

The interface between AlGaAsSb and InP occurred where the bottom DBR and InP heat-current-spreading layer met, as seen in Fig. 1. This interface involved the transition between a quaternary and binary alloy, with no common anions or cations between them. As a result, many different methods for switching from one material to the next could be imagined. Previously, we transitioned from AlGaAsSb to InP by soaking the static AlGaAsSb surface in both As and Sb beams while adjusting the P valve position for InP growth. We then soaked the AlGaAsSb surface under P_2 flux to pump out excess As and Sb for 30 s. InP growth was then initiated. Using this approach (referred to as AsSb soak) occasionally yielded acceptable films, including some of our prior VCL results, but was not sufficiently reproducible for reliable usage. Antimony adatoms present on the static surface tended

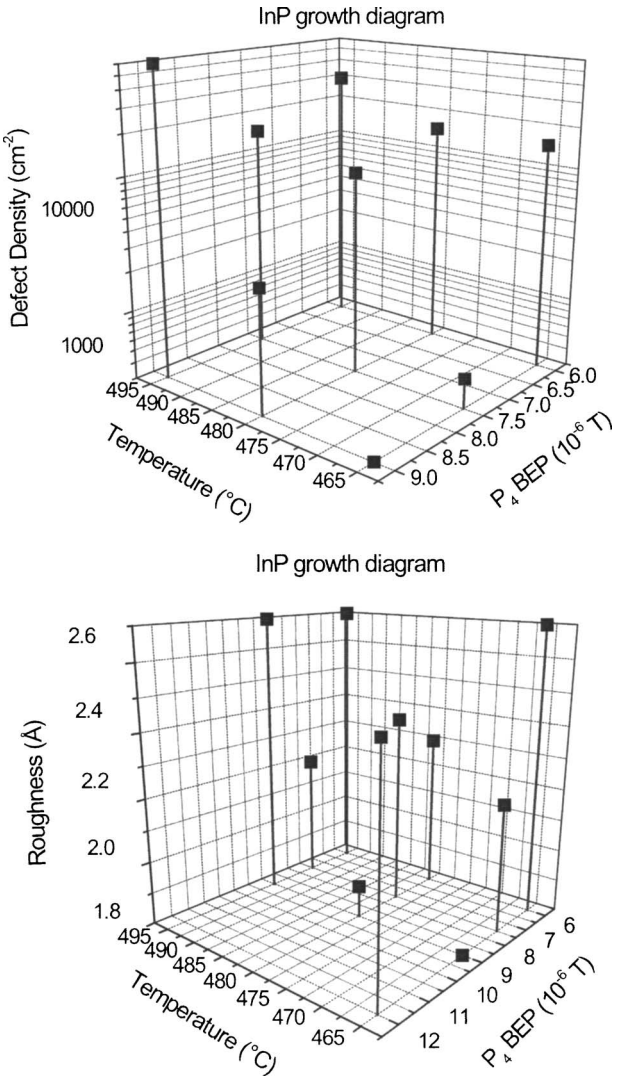

FIG. 2. rms roughness (top) and defect density (bottom) dependence on InP homoepitaxial layers. Growth rate for InP in all cases is 0.15 nm/s.

to remain even with subsequent P_2 soaking, due to the relatively cool growth temperature of 465 °C. This led to the observed defects and roughness. In order to overcome this limitation we developed a transition approach (referred to as P soak) in which P_2 is the only group V species present during the growth pause between AlGaAsSb and InP. This transition used a short initial P_2 soak followed by a thin (2.0 nm) InP buffer layer. This buffer layer was then exposed to the P_2 beam for 60 s to pump out the excess As and Sb still present. Growth of InP continued using the optimized conditions described above. Using this technique we routinely and repeatedly obtained films with low defect density and roughness. In Table I we summarize and compare the two transition methods.

Using this interface transition technique, in conjunction with the optimized AlGaAsSb and InP bulk heteroepitaxy, a full 1310 nm VCL device layer structure was grown. An AFM image of the wafer surface after this 15 μm thick growth is given in Fig. 3. The rms roughness of this surface is 0.31 nm.

TABLE I. Transitions between AlGaAsSb–InP.

AsSb soak	P soak
AlGaAsSb DBR growth	AlGaAsSb DBR growth
Soak AsSb surface with both As_2 and Sb_2 flux—30 s	Soak AsSb surface with only P_2 flux—5 s
Open in shutter, grow according to optimized conditions	Grow 2.0 nm InP buffer layer
	Soak InP buffer layer with P_2 flux—60 s
	Grow remaining InP using optimized conditions
Macroscopic growth results	
Defect density: 5000 cm^{-2}	Defect density: 200 cm^{-2}
rms roughness: 1.5 nm	rms roughness: 0.18 nm

III. VERTICAL CAVITY LASER DEVICE STRUCTURE AND RESULTS

Our 1310 nm VCL structure and design have been detailed elsewhere;[8] the major features are described here, with some of the most pertinent device results provided as well. After MBE growth, the completed all-epitaxial laser structure was fabricated using standard lithographic techniques, with the thin tunnel-junction aperture formed by selectively etching the AlInGaAs with respect to surrounding InP using a solution of citric acid and hydrogen peroxide (10:1 ratio). The devices were then probed on a stage mounted with an InGaAs photodetector, and the light-current-voltage (*L-I-V*) characteristics measured. In Fig. 4 we see *L-I* curves for a range of temperatures, showing continuous-wave (cw) operation up to a maximum of 90 °C. Figure 5 shows the *L-I-V* curves for a device with an aperture diameter of 5 μm at room temperature.

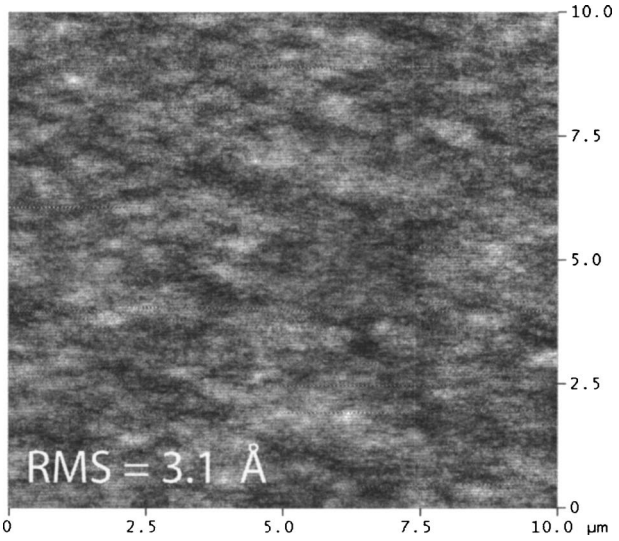

FIG. 3. Atomic-force microscope image of 10×10 μm^2 completed vertical cavity laser layer structure epilayers. The scale in the image is 5 nm. Surface roughness (rms) is 3.1 Å.

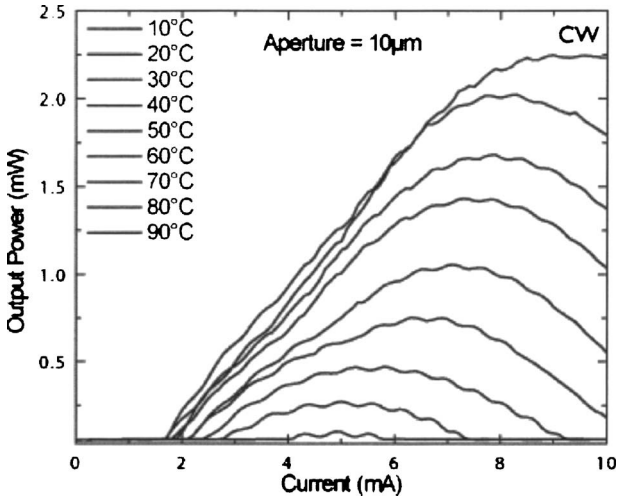

FIG. 4. Light-current curves for a multimode 1310 nm vertical cavity laser operating continuous wave at a range of temperatures. Maximum operating temperature of 90 °C is observed.

This device has single-mode output power greater than 1.0 mW, and differential quantum efficiency of 60%, and other devices exhibited up to 64%. This efficiency is a record for all long-wavelength vertical cavity lasers. The high differential efficiency can be attributed to low excess optical losses in the structure, thanks to the thin tunnel-junction aperture located at the standing wave null of the mode in the optical cavity, along with low free-carrier absorption losses from the mostly *n*-type doping in the structure, and undoped DBRs. The high temperature operation is limited by the active region injection efficiency, which decreased to zero near 120 °C. Rolloff in the output power with drive current is limited by a reduction in injection efficiency with temperature; improvements to the characteristic temperature via redesigning the band structure of the quantum wells and barriers will lead to increased maximum operating temperature for the VCLs. In addition, optimization of the spectral offset between the cavity mode and optical gain peaks should increase the achievable maximum temperature.

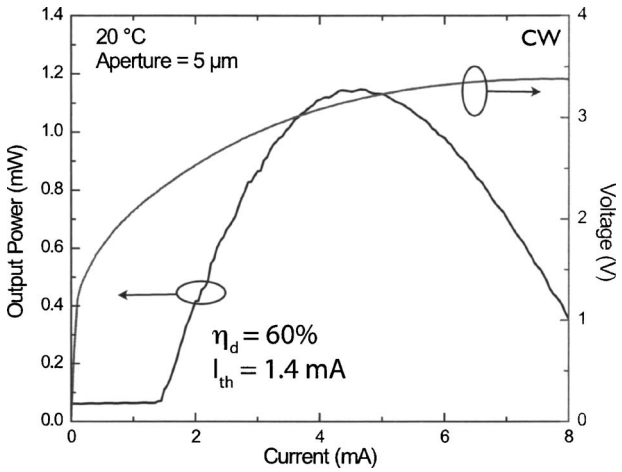

FIG. 5. *L-I-V* curves for a single-mode 1310 nm vertical cavity laser operating continuous wave at room temperature. Maximum output power of 1.1 mW and differential efficiency of 60% are observed.

IV. CONCLUSIONS

Long-wavelength vertical cavity lasers grown all epitaxially on InP substrates can take advantage of AlGaAsSb alloys for highly reflective Bragg mirrors and AlInGaAs alloys for quantum well active regions. The interface between AlGaAsSb and InP has been optimized for minimum defect density and roughness. Growth of complete layer structures with 0.31 nm rms roughness has been demonstrated with low defect density. VCLs at 1310 nm were then fabricated with low-loss thin tunnel-junction apertures for current and optical confinements. Operation at temperatures as high as 90 °C was observed, with single-mode output power above 1.6 mW. Differential quantum efficiency as high as 64% was achieved, a record for long-wavelength vertical cavity lasers.

ACKNOWLEDGMENTS

The authors thank Mr. Geir Myrvågnes for discussion on the AlGaAsSb MBE growth. This work made use of MRL Central Facilities supported by the MRSEC Program of the National Science Foundation under Award No. DMR00-80034 and was funded by NSF under Award No. ECS-0245426.

[1]N. Ueki *et al.*, IEEE Photonics Technol. Lett. **11**, 1539 (1999).
[2]M. Kondow *et al.*, IEEE J. Sel. Top. Quantum Electron. **3**, 719 (1997).
[3]V. Gambin *et al.*, IEEE J. Sel. Top. Quantum Electron. **8**, 794 (2002).
[4]V. Jayaraman *et al.*, IEEE Photonics Technol. Lett. **15**, 1495 (2003).
[5]J. Cheng *et al.*, IEEE Photonics Technol. Lett. **15**, 7 (2005).
[6]R. Shau *et al.*, Electron. Lett. **37**, 1295 (2001).
[7]S. Nakagawa *et al.*, IEEE J. Sel. Top. Quantum Electron. **7**, 224 (2001).
[8]D. Feezell *et al.*, Electron. Lett. **14** (2005).
[9]O. Blum *et al.*, Appl. Phys. Lett. **67**, 3233 (1995).
[10]M. H. M. Reddy *et al.*, Appl. Phys. Lett. **82**, 1329 (2003).